THE JOURNAL OF BIOLOGICAL CHEMISTRY VOL. 285, NO. 15, pp. 11336–11347, April 9, 2010

Rapid Modulation of the Organic Anion Transporting Polypeptide 2B1 (OATP2B1, SLCO2B1) Function by Protein Kinase C-mediated Internalization*[S]

Received for publication, August 19, 2009, and in revised form, February 15, 2010 Published, JBC Papers in Press, February 16, 2010, DOI 10.1074/jbc.M109.056457

Kathleen Köck[‡], Anna Koenen[‡], Bernd Giese[§], Martin Fraunholz[§], Karen May[‡], Werner Siegmund[‡], Elke Hammer[¶], Uwe Völker[¶], Gabriele Jedlitschky[‡], Heyo K. Kroemer[‡1], and Markus Grube[‡]

From the [‡]Department of Pharmacology, Research Center of Pharmacology and Experimental Therapeutics, the [§]Competence Center of Functional Genomics, and the [¶]Interfaculty Institute for Genetics and Functional Genomics, Ernst Moritz Arndt University, 17487 Greifswald, Germany

Members of the organic anion transporting polypeptide (OATP) family are involved in various pharmacological, pathophysiological, and physiological processes, such as hepatic drug uptake, progress of cancer, or transport of hormones. Although variability in expression and function of OATPs has been investigated in detail, data concerning regulation are rather limited. Here, we report a novel mechanism for rapid regulation of OATP2B1 mediated by protein kinase C (PKC) resulting in significant changes of transport activity. PKC activation by the phorbol ester (phorbol 12-myristate 13-acetate, PMA) resulted in increased phosphorylation of OATP2B1 as well as reduced OATP2B1 transport activity with a decrease in V_{max} of E_1S uptake (288 ± 21 (control) *versus* 165 ± 16 pmol/min/mg of protein (PMA)). This effect was sensitive to the PKC inhibitor bisindolylmaleimide I (BIM-I). Confocal microscopy, fluorescence-based internalization assay, and live-cell imaging using green fluorescent protein-tagged OATP2B1 revealed that transport inhibition was due to internalization of the transporter. Furthermore, colocalization with LAMP-2 and chloroquine-sensitive degradation of OATP2B1 suggest that the internalized protein is targeted to a lysosomal degradation pathway. With regard to the underlying mechanism inhibition of caveolin/lipid raft-mediated endocytosis failed to prevent OATP2B1 internalization, whereas inhibition of clathrin-mediated processes blocked OATP2B1 sequestration. However, small interfering RNA-mediated clathrin knock-down affected general trafficking of OATP2B1 and resulted in intracellular accumulation in the absence of PMA. In conclusion, our data demonstrate that OATP2B1 function is regulated by PKC-mediated, clathrin-dependent internalization and followed by lysosomal degradation. Furthermore, internalization could be shown in an *ex vivo* placenta perfusion. Our findings represent a new, rapid mechanism in regulation of human OATPs.

Organic anion transporting polypeptides (OATPs)[2] belong to the solute carrier (SLC)-superfamily, and are involved in the cellular uptake of endo- and exogenous compounds. In general, OATP transporters are expressed in a variety of tissues, but hitherto pharmacological relevance has mainly been studied for the liver-enriched transporters of the OATP1B subclass thereby focusing on hepatocellular drug uptake and elimination.

Several single nucleotide polymorphisms have been identified within the liver-enriched OATP1B1 transporter with impact on transport function (1, 2). Some of those single nucleotide polymorphisms are commonly occurring and translate into alterations of drug disposition in humans. Due to reduced hepatic accumulation of OATP1B1 substrates such as statins, which exert their pharmacological function on the 3-hydroxy-methylglutaryl-coenzyme A reductase in hepatocytes, carriers of certain variants appear to exhibit decreased cholesterol-lowering efficacy (3). Accordingly, subjects carrying these OATP1B1 variants have an enhanced risk of myotoxic side effects (4–6).

In addition to these pharmacokinetic effects, increasing evidence suggests that members of the OATP family are associated with cancer development and progression. OATP1B3, which is mainly expressed in hepatocytes under normal conditions, was recently reported to be overexpressed in prostatic cancer as well as colorectal adenocarcinomas. In prostatic cancer, the OATP1B3 334GG/699AA haplotype was associated with a prolonged median survival, which was suggested to be due to the impaired testosterone transport of this variant (7). In colorectal cancer cell lines, OATP1B3 expression diminished drug-induced apoptosis by reducing the transcriptional activity of p53. Overexpression of a non-functional OATP1B3 variant neither resulted in anti-apoptosis nor affected p53 transcriptional activity suggesting that this effect is associated with transport activity (8).

In contrast to the predominant liver-enriched expression of OATP1B1 and -1B3, other members of the OATP family dem-

* This work was supported by Deutsche Forschungsgemeinschaft Grant GR 3375/1-1.

[S] The on-line version of this article (available at http://www.jbc.org) contains supplemental Figs. S1–S3 and Movie 1.

[1] To whom correspondence should be addressed: Friedrich-Loeffler-Str. 23d, 17487 Greifswald, Germany. Tel.: 49-3834-865630; Fax: 49-3834-865631; E-mail: kroemer@uni-greifswald.de.

[2] The abbreviations used are: OATP, organic anion transporting polypeptide; BIM-I, bisindolylmaleimide-I; CHC, clathrin heavy chain; CHL, chloroquine; Cav1, caveolin-1; DHEAS, dehydroepiandrosterone sulfate; E_2G, estradiol 17β-glucuronide; E_1S, estrone-3-sulfate; PMA, phorbol 12-myristate 13-acetate; PK, protein kinase; GFP, green fluorescent protein; hTfR, human transferrin receptor; PBS, phosphate-buffered saline; MDCK cell, Madin-Darby canine kidney cell; DMSO, dimethyl sulfoxide; siRNA, small interfering RNA; SLC, solute carrier.

onstrate a wide tissue expression (for review, see Ref. 9). For example, OATP2B1 is highly expressed in liver, intestine, heart, placenta, and platelets (10–15) and acts as a cellular uptake transporter for drugs including atorvastatin, pravastatin, aliskiren, or glibenclamide as well as endogenous compounds such as estrone-3-sulfate (E_1S), dehydroepiandrosterone sulfate (DHEAS), and pregnenolone sulfate (12–14, 16–20). Although clinical studies providing evidence of a pharmacokinetic impact of OATP2B1 are still limited, its expression in organs like placenta or mammary gland suggests an important role in uptake of precursor molecules for steroid hormone synthesis.

Although the impact of inherited modifications of OATPs has been studied in detail, functional modulation by altered expression or other modifications have been addressed only in few studies. Recently, gender-dependent differences and regulation of OATP expression by nuclear receptors (*e.g.* farnesoid X, liver X, and pregnane X receptor) have been described for human as well as rodent OATPs (21–24). These effects are tightly controlled on a transcriptional level, dependent on mRNA as well as protein turnover and hence represent a slow mode of response. We hypothesize that physiological mechanisms exist that enable a fast, local and transient adaptation of OATP expression to altered external conditions to guarantee cellular homoeostasis. Several signaling pathways comprising different second messenger and protein kinase/phosphatase systems have been identified to affect protein modification. So far, activation of protein kinase A or C (PKA and PKC, respectively) has been associated with alterations of transporter function and/or their presence in the plasma membrane as their primary site of action. For example, such short-term regulation has been reported for the human organic anion transporter 1 (OAT1); here, PKC-induced down-regulation of transport activity was achieved through carrier retrieval (25, 26). In the case of OATPs such rapid effects have been described for rodent proteins (27). Recently, PKA activation has been shown to stimulate membrane localization of a green fluorescent protein (GFP)-tagged OATP1B1 and to enhance E_1S uptake by ~20% (28).

In the present study we describe a rapid regulation of OATP2B1 function and localization by PKC activation in MDCKII-OATP2B1 and Caco-2 cells as well as human placenta. Fast intracellular accumulation of the transporter resulting in altered substrate kinetics was confirmed by immunofluorescence and live-cell imaging of GFP-tagged OATP2B1. This process was mediated by clathrin-dependent retrieval into intracellular vesicles, and subsequent lysosomal degradation of OATP2B1.

EXPERIMENTAL PROCEDURES

Cell Culture and Materials—Madin-Darby canine kidney (MDCKII) cells were stably transfected with human OATP2B1 and characterized as described previously (17). MDCKII-OATP2B1, the parental cell line as well as Caco-2 cells were grown in 75-cm^2 cell culture flasks in Dulbecco's modified Eagle's medium supplemented with 2 mM L-glutamine, 1% minimal essential medium nonessential amino acids, 10% fetal calf serum, 100 units/ml of penicillin, and 100 μg/ml of streptomycin. Except for the experiments, the transfected cell line was maintained in medium containing 350 μg/ml of hygromycin B. Caco-2 cells were seeded at an initial density of 6×10^4 cells/cm^2 and medium was changed every other day. Cells were incubated at 37 °C in a humidified atmosphere containing 5% CO_2.

[^{3}H]E_1S (specific activity, 50 Ci/mmol) and [^{3}H]DHEAS (specific activity, 63 Ci/mmol) were obtained from Hartmann Analytic (Braunschweig, Germany) and Biotrend (Cologne, Germany), respectively. Bisindolylmaleimide-I (BIM-I) was from Tocris (Bristol, United Kingdom), PMA was from Alexis Biochemicals (San Diego, CA). Sulfo-NHS-SS-biotin and fluorescein isothiocyanate-labeled streptavidin were purchased from ThermoFisher Scientific (Rockford, IL). All other chemicals were purchased from standard suppliers. Mouse monoclonal anti-caveolin-1 and anti-E-cadherin antibodies were from BD Bioscience, anti-phospho-Ser/Thr/Tyr from Anaspec (San Jose, CA), anti-glyceraldehyde-3-phosphate dehydrogenase from Biodesign (Saco, MA), anti-clathrin heavy chain (CHC) monoclonal antibody TD.1 and anti-LAMP-2 were from Santa Cruz (Santa Cruz, CA). For detection of OATP2B1 a guinea pig polyclonal antibody raised against amino acids 25–41 of OATP2B1 (OATP2B1/gp) as well as a rabbit polyclonal antibody raised against the 15 C-terminal amino acids of OATP2B1 (OATP2B1/r) were used.

Cloning and Transfection—The transporter cDNA fragment from the pcDNA3.1/Hygro-OATP2B1-construct, which has previously been described (29), was amplified using the following primers containing NheI and SacII cleavage sites (bold): forward primer (SacII) 5′-tgct**ccgcgg**ctgcactccagcagtcatg and reverse primer (NheI) 5′-agac**gctagc**cactcgggaatcctctgg and cloned to the N terminus of the GFP in the mammalian expression vector pQBI-25-fC3 (MP Biomedicals Europe, Illkirch, France). The sequence was verified against the reference sequence (accession number AB026256) and MDCKII cells were transfected with the OATP2B1/vector-construct using FuGENE 6 Transfection Reagent (Roche Applied Science). Cells were selected for antibiotic resistance using 0.6 mg/ml of neomycin (Invitrogen) and resistant cell clones were characterized for OATP2B1-GFP expression using immunofluorescence microscopy.

To generate a phosphorylation site defective pcDNA3.1/Hygro-OATP2B1 construct, amino acids Thr^{22}, Thr^{28}, Ser^{34}, Ser^{43}, Thr^{318}, Ser^{320}, Ser^{328}, Ser^{330}, Ser^{333}, Ser^{337}, Thr^{338}, Thr^{367}, Ser^{685}, Ser^{687}, Ser^{688}, Ser^{698}, and Ser^{707} were simultaneously substituted by alanine using a multisite-directed mutagenesis kit (Stratagene, La Jolla, CA).

The human transferrin receptor (hTfR) was amplified from human placenta-derived cDNA using primers 5′-atgatggatcaagctagatca (forward primer) and 5′-ttaaaactcattgtcaatgtcc (reverse primer) and cloned to the N terminus of yellow fluorescent protein into the pcDNA6.2-YFP vector (Invitrogen). The sequence was verified against the reference sequence (accession number NM_003234.2). This vector construct was transiently transfected into MDCKII-OATP2B1 cells using Lipofectamine 2000 (Invitrogen).

Transport Assays—For transport studies cells were seeded in 24-well dishes and cultured to confluence. Cells were preincubated for the times indicated in the respective sections or figure legends at 37 °C with 500 μl of medium/well containing pro-

tein kinase activators, inhibitors, or internalization inhibitors. Afterward the medium was removed, cells were washed twice with prewarmed PBS, and incubated at 37 °C with a transport buffer containing 140 mM $NaCl_2$, 5 mM KCl, 1 mM KH_2PO_4, 1.5 mM $CaCl_2$, 5 mM glucose, and 12.5 mM HEPES (pH 7.4) and the respective substances. At specified time points the transport buffer was rapidly aspirated and cells were washed four times with ice-cold PBS. Cells were solubilized in 0.2% SDS containing 0.5 mM EDTA, an aliquot was dissolved in 2 ml of scintillation mixture (Rotiszint, Roth, Karlsruhe, Germany) and measured in a scintillation β-counter (type 1409, LKB-Wallac, Turku, Finland). Determination of kinetic parameters (K_m and V_{max}) of E_1S uptake in the presence or absence of PMA was obtained by incubating the cells with increasing concentrations of E_1S.

Immunohistological Analyses—For immunohistological analyses cells were grown to confluence on coverslips in 12-well plates. Cells were fixed for 10 min with ethanol (99.9%), permeabilized with Triton X-100 (0.1%) for 5 min at room temperature, and blocked with 5% fetal calf serum in PBS. Staining was carried out using the OATP2B1/r antibody for 2 h at room temperature as described previously (17). The secondary AlexaFluor® 488-conjugated goat anti-rabbit antibody (Invitrogen) was used for fluorescence detection. For LAMP-2-costaining, cells were incubated with the OATP2B1/r (1:200) and LAMP-2 (1:50) antibodies. The secondary antibodies used were goat anti-rabbit AlexaFluor® 568 and chicken anti-rabbit AlexaFluor 488 (1:200 each). The cells were washed as mentioned before and mounted on glass slides with Fluorescent Mounting Medium (DakoCytomation, Carpinteria, CA).

Phosphorylation Assay—Following treatment, cells were lysed in RIPA buffer (1% (w/w) Nonidet P-40, 1% (w/v) sodium deoxycholate, 0.1% (w/v) SDS, 0.15 M NaCl, 0.01 M sodium phosphate, pH 7.2, 2 mM EDTA, 1.0 mM sodium vanadate, 0.1 mM phenylmethylsulfonyl fluoride, 0.3 μM aprotinin, 0.1 μM pepstatin and phosphatase inhibitor mixture 1 (Sigma)) for 1 h on ice. Lysates were precleared with Fast-Flow protein G-Sepharose (100 μl/ml of cell lysate) for 10 min, followed by immunoprecipitation of 100 μg of protein using the OATP2B1/gp antibody and Fast-Flow protein G-Sepharose. The complexes were washed with RIPA buffer and proteins were eluted with 4× Laemmli before subjecting the samples to a 7.5% SDS-polyacrylamide gel. Western blotting was performed using an anti-phospho-Ser/Thr/Tyr antibody as well as the OATP2B1/r antibody. For quantitation, densitometric values of the phosphorylated protein were normalized to the amount of immunoblotted OATP2B1.

Time-lapse Analyses—OATP2B1-GFP-expressing cells were seeded into LabTekII™ chambered coverglass (Nunc, Wiesbaden, Germany) and incubated in normal tissue culture medium in a Pekon incubator (Pekon, Germany) at 37 °C in an atmosphere containing 5% CO_2. Imaging was performed with the Zeiss LSM 510 confocal laser scanning microscope (Carl Zeiss GmbH, Jena, Germany) equipped with an argon-ion laser. Cells were examined with a 63 × 1.2 NA Zeiss water immersion c-apochromate objective in phenol red-free medium. GFP fluorescence was detected using the 488 nm emission line of the argon laser. The beampath contained a 488-nm main dichroic mirror and a 505-nm longpass filter. The images represent 0.8-μm thick confocal slices. For time-lapse experiments sequential images were acquired every minute.

Placenta Perfusion—Immediately after delivery, the fetal and maternal sides of three placentas were perfused as described recently (30). The flow rate was 12 ml/min in the maternal circuit and 4 ml/min in the fetal circuit with an arterial pressure between 25 and 40 mm Hg. The total perfusion volume in each circuit was 140 ml. Following an open loop perfusion for 30 min to remove blood, a close-loop perfusion for 1 h was performed for stabilization and detection of leakage or noncongruent maternal and fetal perfusion. Afterward, 100 nM PMA dissolved in circulation medium was given to the maternal and fetal circulation and perfused for 1 h. Tissue samples were dissected from an unperfused cotyledon before and from the perfused cotyledon after perfusion with PMA. After staining with the OATP2B1/r and E-cadherin antibody the colocalization coefficient of OATP2B1 with E-cadherin in confocal images was calculated by dividing the number of pixels of the OATP2B1 channel that colocalized with signals of the E-cadherin channel by the total number of OATP2B1 pixels. For qualitative analysis colocalizing pixels of both channels were subtracted from the original OATP2B1 signal using the LSM Image Browser (Carl Zeiss GmbH, Jena, Germany) and the resulting images were presented in false color.

Cell Surface Biotinylation and Fluorescence-based Internalization Assay—The origin of the internalized OATP2B1 was investigated using the membrane-impermeable sulfo-NHS-SS-biotin. For cell surface biotinylation, cells were seeded in 12-well dishes, treated with PMA or DMSO, washed three times with ice-cold PBS/CM (138 mM NaCl, 2.7 mM KCl, 1.5 mM KH_2PO_4, 0.1 mM $CaCl_2$, and 1 mM $MgCl_2$), and incubated with sulfo-NHS-SS-biotin (1 mg/ml in PBS/CM) at 4 °C. After 1 h, each well was rinsed three times with PBS/CM containing 100 mM glycine and then incubated for 20 min in the same solution at 4 °C to ensure complete quenching of unreacted biotin. Afterward, cells were lysed for 1 h with buffer containing 10 mM Tris, 150 mM NaCl, 1 mM EDTA, 0.1% SDS, 1% Triton X-100 (pH 7.4). Following centrifugation for 5 min at 13,000 × *g*, 100 μg of the supernatant protein was incubated with 33 μl of Neutravidin beads (ThermoScientific) overnight in a total volume of 133 μl. After three washings with lysis buffer, proteins were eluted by incubation with 4× Laemmli buffer for 10 min at 95 °C and subjected to Western blot analysis.

For the fluorescence-based internalization assay, biotinylated cells were incubated in prewarmed medium containing either DMSO or PMA for 1 h at 37 °C to initiate internalization. Residual cell surface biotin was cleaved off by incubating the cells three times for 20 min at 4 °C with glutathione stripping solution (50 mM glutathione, 75 mM NaCl, 1 mM EDTA, 1% bovine serum albumin, 0.75% (v/v) 10 N NaOH). Bovine serum albumin and NaOH were added just before use. Afterward, cells were rinsed three times with ice-cold PBS. Efficiency of stripping was determined on biotinylated cells incubated in parallel on ice. Following fixation with ethanol (99.9%) and permeabilization with Triton X-100 (0.1%) cells were probed with fluorescein isothiocyanate-labeled streptavidin at a concentration of 40 μg/ml (30 min at 37 °C) and the OATP2B1/r antibody.

Western Blot Analyses—Samples were lysed in a buffer containing 50 mM Tris, 100 mM NaCl, 0.1% Triton X-100, and 5 mM EDTA supplemented with protease inhibitors (0.1 mM phenylmethylsulfonyl fluoride, 0.3 μM aprotinin, and 0.1 μM pepstatin). After 1 h on ice and occasional vortexing, samples were centrifuged at 3,000 × *g* for 5 min to remove cell debris. After determination of the protein content using the BCA method equal amounts of protein were loaded on 7.5 or 12% SDS-polyacrylamide gels. After separation and transfer to polyvinylidene membranes, blots were probed with OATP2B1/r (31) (1:2000), Cav1 (1:1000), CHC (1:1000), glyceraldehyde-3-phosphate dehydrogenase (1:1000), or phospho-Ser/Thr/Tyr (1:200) antibodies. Immunoreactivity was visualized using an enhanced chemiluminescence system (GE Healthcare). To block lysosomal acidification and lysosomal protease activity the cells were cultured in the presence of 100 μM chloroquine in regular medium.

Clathrin and Caveolin Knock-down—Cells were transfected using siRNA duplexes (Invitrogen) directed against canine caveolin-1 (Gi:50979109; Cav1_314, AUUGGGAUGCCAAAGAGGGTT; Cav1_385, GCAGUUGUGCCGUGCAUUATT; and Cav1_503, AUGUUGAUGCGGAUAUUGCTT) and canine clathrin heavy chain (Gi:73966640; CHC_2077, GCAGUUUGCCCAAAUGUUATT). siRNA (20 nM each for caveolin-1 and 45 nM for CHC) was transfected with Lipofectamine™ RNAiMAX applying the reverse transfection protocol.

Inhibition of Clathrin- or Caveolin/Lipid Raft-mediated Endocytosis—MDCKII-OATP2B1 as well as hTfR-transfected MDCKII-OATP2B1 cells were subjected to various conditions inhibiting clathrin- or caveolae/lipid raft-mediated endocytosis. To block internalization mediated via clathrin-dependent mechanisms cells were preincubated with either hypertonic medium (0.45 M sucrose in culture medium) for 30 min or with 10 mM acetic acid in culture medium (pH 5.0) for 10 min as described previously (32). To disrupt caveolin-mediated endocytosis, preincubation with either filipin (5 μg/ml) or nystatin (25 μM) for 30 min was performed (33). Following these treatments, cells were either incubated with DMSO or PMA in medium for 1 h and immunostained as described above.

In Silico Analyses, Statistics, and Imaging Analysis—Phosphorylation sites of the OATP2B1 were predicted using phosphorylation site prediction programs NetPhos 2.0 (34), Disphos1.3 (35), and GPS2.1 (36). Amino acids located intracellularly with a score higher than 0.5 (NetPhos 2.0, Disphos) as well as amino acids identified in GPS prediction using a high threshold were investigated further.

Experimental data are presented as mean ± standard deviation (S.D.). Graphs and statistical analyses were performed with Excel or GraphPad Prism 5.01. To determine statistical significance Student's *t* test was used. For phosphorylation experiments the Wilcoxon signed-rank test was performed. When more than two groups were present, data were compared by one-way analysis of variance using Bonferroni's multiple comparison test. Differences were considered significant at $p < 0.05$. The kinetic parameters K_m and V_{max} were determined with GraphPad Prism 5.01 using nonlinear regression analysis employing the following equation: $Y = (V_{max} \times X)/(K_m + X)$, where Y is transport velocity per time and X is substrate concentration. For determination of internalization the ratio between intracellular and plasma membrane expression was calculated by definition of regions of interest in the LSM Image Browser and computing of the mean intensities.

RESULTS

Effect of Protein Kinase Activators on OATP2B1 Function—To evaluate the influence of PKA and PKC activation on OATP2B1-mediated transport, activators of the respective kinases were used. For this purpose MDCKII-OATP2B1 cells were treated with cell-permeable PKA activators 8-bromo-cAMP and dibutyryl-cAMP (100 μM each) as well as the indirect PKA activator forskolin (10 μM) and the PKC activator PMA (10 μM) for 1 h. After washing with prewarmed PBS, [^{3}H]E_1S uptake (1 μM, 0.25 μCi/ml of incubation buffer, 5 min) was measured. Activation of PKC by 10 μM PMA reduced the OATP2B1-mediated E_1S uptake to 37 ± 1% of control, whereas PKA activation had no effect (Fig. 1*A*), even in concentrations ranging from 0.316 μM to 1 mM (data not shown). Similar results were obtained for [^{3}H]DHEAS uptake (data not shown).

To further analyze the inhibitory effect of PMA on OATP2B1-mediated transport, MDCKII-OATP2B1 as well as MDCKII cells were incubated with PMA concentrations ranging from 10 pM to 10 μM. In OATP2B1-overexpressing cells, PMA suppressed the E_1S uptake in a concentration-dependent manner, whereas transport into control cells remained unchanged. The half-maximal inhibitory concentration (IC_{50}) of PMA was calculated to 7.7 ± 4.3 nM for the E_1S (Fig. 1*B*) and 1.3 ± 1.1 nM for DHEAS transport (data not shown). Incubation of MDCKII-OATP2B1 cells with 100 nM PMA for various time intervals (5 min to 24 h) prior to the uptake assay revealed a time-dependent effect. E_1S uptake was significantly reduced in as little as 20 min with a maximal effect of 83.2 ± 2.2% inhibition after 2 h. Incubation periods exceeding this time point resulted in a lower inhibition rate: cells exposed to PMA for 24 h exhibited an E_1S transport of 50 ± 2% compared with control (Fig. 1*C*). To test whether the PMA effect is reversible, cells were treated with PMA for only 1 h followed by incubation with PMA-free medium for the indicated times. Although up to 11.5 h no difference was observed compared with cells incubated in the continuous presence of PMA, transport was restored to 100 ± 8% (*versus* non-PMA treated cells) after 26.5 h (Fig. 1*C*, *dotted line*).

To further determine whether the PMA-induced transport inhibition was PKC-mediated, cells were preincubated with the PKC inhibitor BIM-I (1 μM) 20 min before and during PMA (100 nM) treatment. Although BIM-I incubation alone did not affect OATP2B1 transport activity, coincubation of BIM-I and PMA resulted in almost complete reversal of the PMA-mediated suppression of OATP2B1-mediated E_1S uptake (BIM-I alone 97 ± 24%; PMA alone 16 ± 3%; PMA plus BIM-I 78 ± 9%; control 100 ± 15%, $n = 3$) (Fig. 1*D*).

Kinetic Analyses and Immunofluorescence—PKC activation may inhibit OATP2B1 function through changes of substrate affinity, modulation of protein surface expression, and/or altered turnover rate. To elucidate the underlying mechanism, we determined K_m and V_{max} for E_1S uptake in the presence and

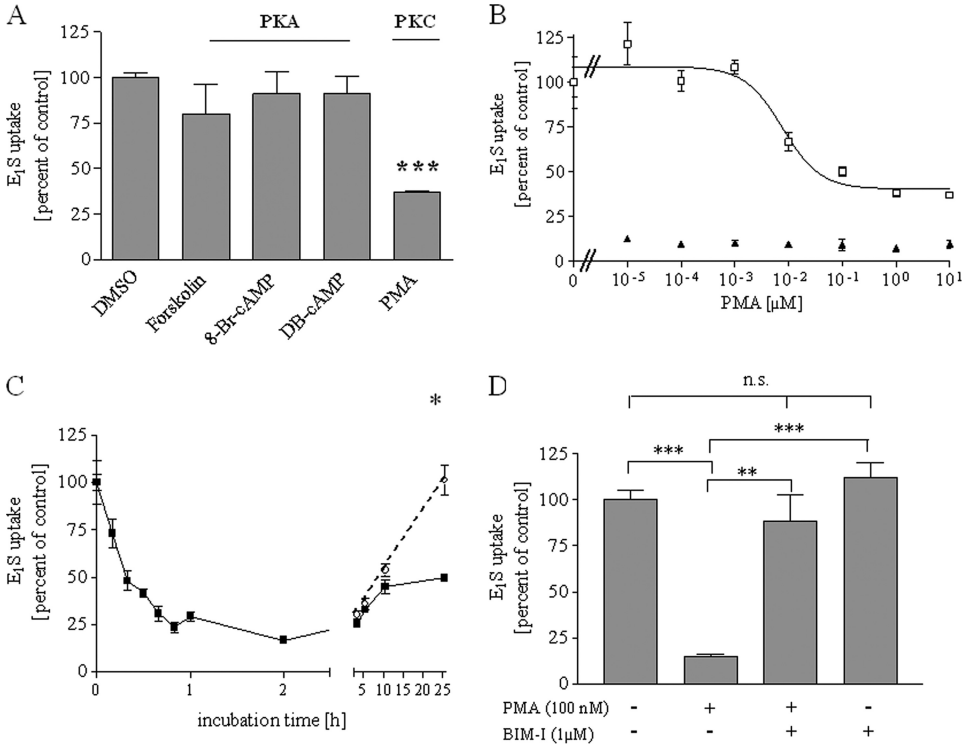

FIGURE 1. **Influence of PK activation on OATP2B1-mediated E_1S uptake.** *A*, uptake of [^{3}H]E_1S (0.25 μCi/ml, 1 μM, 5 min) in MDCKII-OATP2B1 cells was determined after a 1-h incubation with solvent (0.1% DMSO), 10 μM forskolin, 100 μM 8-bromo-cAMP (*8-Br-cAMP*), 100 μM dibutyryl-cAMP (*DB-cAMP*), and 10 μM PMA at 37 °C. Statistical significance against vehicle-incubated cells was determined by Student's *t* test. *B*, concentration dependence of the PMA effect: MDCKII (▲) and MDCKII-OATP2B1 (□) cells were incubated in medium supplemented with increasing concentrations of PMA (10 pM to 10 μM) for 1 h before measuring [^{3}H]E_1S uptake. *C*, time dependence and reversibility of the PMA effect: uptake of [^{3}H]E_1S was measured after treatment with 100 nM PMA (■) for 0–26.5 h or after incubation with PMA for 1 h followed by incubation with PMA-free medium (○) ($n = 3$ of three independent experiments). *D*, involvement of PKC in down-regulation of OATP2B1-mediated E_1S transport: MDCKII-OATP2B1 cells were incubated with the PKC inhibitor BIM-I (1 μM) or control (0.1% DMSO) 20 min prior and during incubation with 100 nM PMA or 0.1% DMSO for 60 min followed by [^{3}H]E_1S accumulation assay. Data are shown as percentages of the MDCKII-OATP2B1 cells incubated in the absence of PMA. Data were compared by one-way analysis of variance using Bonferroni's multiple comparison test. Values of all experiments represent mean + S.D., $n = 3$. **, $p < 0.01$; *** $p < 0.001$. *n.s.*, not significant.

absence of PMA (100 nM). Nonlinear regression analysis revealed that PMA treatment significantly reduced V_{max} from 288 ± 20.7 pmol/min/mg of protein (control) to 164.5 ± 15.8 pmol/min/mg of protein (PMA), whereas the affinity toward the transporter was not significantly altered (9.5 ± 1.5 and 13.2 ± 2.6 μM, respectively), suggesting that the observed effects might be due to an altered OATP2B1 plasma membrane expression (supplemental Fig. S1).

Therefore, we analyzed the subcellular localization of OATP2B1. Indeed, incubation with PMA led to a redistribution of OATP2B1 to subcellular compartments. Although staining of MDCKII-OATP2B1 in the absence of PMA revealed a strong basolateral signal, which was still present after a 10-min incubation with 100 nM PMA, the transporter was also detected within intracellular vesicles after a 1-h incubation (Fig. 2, *A–C*). Prolonged incubation periods up to 72 h resulted in a decline of intracellular OATP2B1 and enhanced plasma membrane *versus* intracellular localization (supplemental Fig. S2).

To exclude generalized effects on plasma membrane proteins we co-stained E-cadherin, an adhesion molecule mainly expressed in the basolateral plasma membrane of MDCKII cells. Quantitation of immunofluoresence revealed that there is a 3-fold increase in intracellular OATP2B1 after a 1-h incubation. For E-cadherin we observed a slight increase in intracellular localization following PKC activation; however, this did not reach statistical significance (Fig. 2, *D–F*).

In accordance with transport experiments (see Fig. 1*D*), we could verify the involvement of PKC in enhanced intracellular accumulation mediated by PMA. Incubation with 1 μM BIM-I prior to and during PMA treatment prevented intracellular retrieval of OATP2B1, whereas BIM-I alone had no effect on the localization of the protein (supplemental Fig. S3).

Establishment of a GFP-OATP2B1-expressing Cell Line and Time-lapse Analysis—To further analyze the altered localization of OATP2B1 in response to PKC stimulation, a stable cell line overexpressing GFP-tagged OATP2B1 was established by transfection of MDCKII cells with the OATP2B1-GFP pQBI vector construct and subsequent neomycin selection. The OATP2B1-GFP fusion protein did not differ from the native OATP2B1 protein with regard to localization and apparent K_m values (data not shown). Using time-lapse analysis we demonstrate enhanced retrieval of OATP2B1 into intracellular vesicles starting around 15 min after addition of 100 nM PMA. Live-cell images thus confirmed the effect of PMA on altered OATP2B1 localization obtained by immunofluorescence (see Fig. 2*G* for video snapshots). A time-lapse analysis of this process is provided as supplemental Movie S1.

Internalization of OATP2B1 in Caco-2 Cells—To exclude that the observed processes are artifacts of the overexpression, Caco-2 cells, which endogenously express OATP2B1, were subjected to PMA treatment. After 30 min a significant amount of protein resided intracellularly, whereas 1 h of incubation with PMA resulted in nearly complete intracellular accumulation of OATP2B1. Control-treated cells exhibited a strong expression of OATP2B1 in the plasma membrane (Fig. 2, *H–J*).

Internalization of OATP2B1 in a Placenta Perfusion Model—To answer the question whether PKC-mediated OATP2B1 internalization also plays a role in the biological system, we performed human placenta perfusion studies, a model system that is often used to investigate feto-maternal drug transport and vice versa (30). Using this system we could demonstrate an internalization of OATP2B1 following PMA perfusion (Fig. 3). Quantitation of immunofluorescence of three independent experiments revealed a significant decrease of the colocaliza-

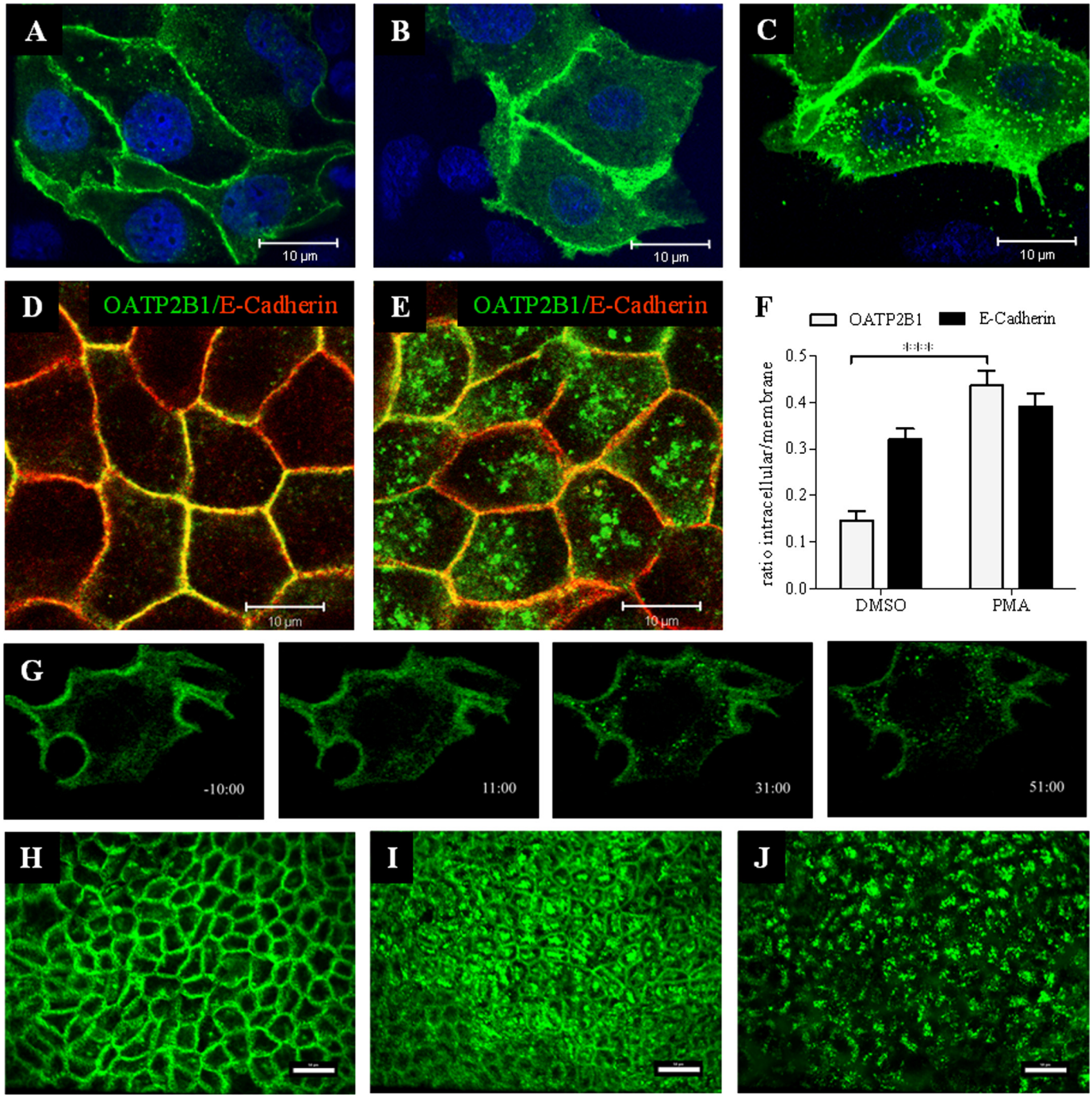

FIGURE 2. **PMA-induced internalization of OATP2B1 in MDCKII-OATP2B1 and Caco-2 cells.** *A–C*, MDCKII-OATP2B1 cells were treated with 100 nM PMA for 0 (*A*), 10 (*B*), and 60 min (*C*), fixed, and probed with the OATP2B1/r antibody as described under "Experimental Procedures." *D–F*, DMSO (*D*)- and PMA (*E*)-treated cells were probed for OATP2B1 (*green*) and E-cadherin (*red*) and expression was quantified for plasma membrane and cytosolic localization (*F*). Values of quantitation are shown as the ratio between intracellular and plasma membrane expression (mean ± S.D., $n = 18$ cells). ***, $p < 0.001$. *G*, time course of PMA-mediated internalization of GFP-tagged OATP2B1 in MDCKII cells. Live-cell confocal imaging implies internalization of the protein after stimulation with 100 nM PMA. Fluorescence of GFP was recorded as described under "Experimental Procedures." The "zero" time point indicates the addition of PMA to the cell culture medium. Data are representative for at least three independent experiments. The complete time lapse is provided in supplemental Movie 1. *H–J*, Caco-2 cells were incubated with 100 nM PMA for 0 (*H*), 30 (*I*), and 60 min (*J*), fixed, and probed with the OATP2B1/r antibody. The *bar* represents 50 μm.

tion coefficient of OATP2B1 with the basolateral membrane protein E-cadherin from 0.67 ± 0.16 (pre-perfusion) to 0.38 ± 0.14 (PMA).

Phosphorylation Analyses—To test whether internalization is accompanied by OATP2B1 phosphorylation, MDCKII-OATP2B1 cells were treated with PMA or DMSO, respectively, and subjected to immunoprecipitation and Western blot analyses. To quantify the level of OATP2B1 phosphorylation, the densitometric values of the phosphorylated protein were normalized to the whole amount of OATP2B1. These analyses revealed a basal phosphorylation of OATP2B1, however, PMA treatment increased the phosphorylation about 2-fold ($p <$

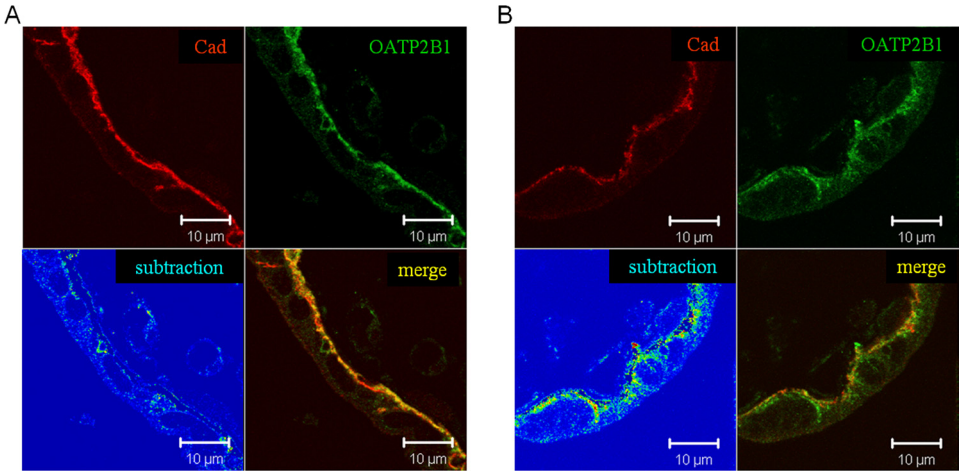

FIGURE 3. **PMA-induced internalization of OATP2B1 in human placenta.** Three human placentas were perfused with 100 nM PMA in fetal and maternal circulation as described under "Experimental Procedures." Paraffin-embedded tissue sections before (*A*) and after (*B*) PMA perfusion were probed with the OATP2B1/r and E-cadherin (*Cad*) antibody (1:200 and 1:1000, respectively). OATP2B1 is given in *green*, E-cadherin in *red*. In the merge colocalized pixels of OATP2B1 and E-cadherin are highlighted in *yellow*. In the subtraction mode, OATP2B1 pixels that colocalized with E-cadherin pixels were subtracted from the original OATP2B1 signal. The resulting OATP2B1 signal is presented in false color from *blue to red* (low *versus* high intensity, respectively). Note the strong intracellular signal of OATB2B1 in the subtraction channel after PMA stimulation (*B*). Data are representative of at least three independent experiments.

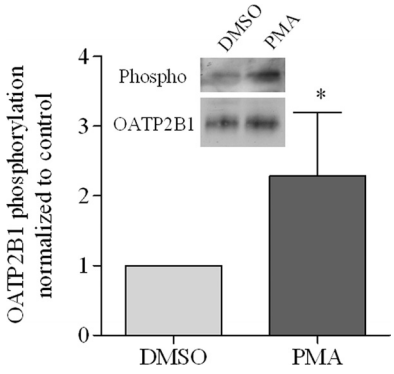

FIGURE 4. **Effect of PMA on OATP2B1 phosphorylation.** For detection of phosphorylated OATP2B1, MDCKII-OATP2B1 were treated with PMA (100 nM) or DMSO, respectively, and subjected to immunoprecipitation using the OATP2B1/gp antibody. Western blot was probed with an antibody against phospho-Tyr/Thr/Ser and OATP2B1/r. Quantitation of phosphorylation was performed as described under "Experimental Procedures." Blots are representative for five independent experiments; quantitation data represent the mean + S.D. of all experiments. Wilcoxon signed-rank test was used to determine statistical significance. *, $p < 0.05$.

0.05) (Fig. 4). Because these studies rely on the specificity of immunoprecipitation we also performed additional experiments with control antisera and omission of the immunoprecipitating antibody. In these experiments neither OATP2B1 nor phosphorylated protein could be detected (data not shown).

To demonstrate an association between phosphorylation and internalization, 17 predicted phosphorylation sites were simultaneously mutated to alanine. However, this construct did not demonstrate an altered response to PKC activation by PMA (data not shown), suggesting that phosphorylation at these sites is not a prerequisite for OATP2B1 internalization.

Sequestration of OATP2B1 from the Cell Surface—Next, we determined whether OATP2B1 is sequestered from the cell surface or if its intracellular accumulation is a result of decreased trafficking toward the plasma membrane. Therefore, a surface biotinylation assay as well as a fluorescence-based internalization assay was performed.

Biotinylation of cell surface proteins followed by purification of biotinylated proteins and OATP2B1 Western blot analysis correlated with the inhibition of transport activity and revealed a time-dependent decrease in the plasma membrane expression of OATP2B1 (Fig. 5*A*). To distinguish between cell surface sequestration and decreased cell surface trafficking a fluorescence-based internalization assay was performed. Therefore, MDCKII-OATP2B1 as well as Caco-2 cells were reversibly biotinylated with Sulfo-NHS-SS-biotin. After treatment with PMA or DMSO residual cell surface biotin was cleaved off using glutathione. Following fixation, biotin as well as OATP2B1 were stained using fluorescein isothiocyanate-labeled streptavidin or a fluorochrome-labeled secondary antibody, respectively. As expected, OATP2B1 was localized at the plasma membrane in DMSO-treated MDCKII-OATP2B1 as well as Caco-2 cells, whereas biotinylated proteins were exclusively found intracellularly. In PMA-treated cells, OATP2B1 and biotinylated protein colocalized intracellularly in both cell lines suggesting a sequestration from the plasma membrane (Fig. 5*B*).

Protein Degradation—After internalization membrane proteins either recycle back to the plasma membrane or are targeted to lysosomal or proteosomal degradation (37). To analyze the fate of the internalized OATP2B1 we tested for colocalization with lysosomes. Therefore, PMA-treated cells were stained for OATP2B1 and the lysosomal marker LAMP-2. The observed colocalization of both proteins suggests a lysosomal degradation of OATP2B1 (Fig. 5*C*). Indeed, Western blot analysis revealed a decline in the protein amount after incubation with PMA: after 4 h a marked decrease of OATP2B1 in PMA-treated cells compared with 0 h and control cells was observed. In addition, cotreatment with chloroquine, which disrupts the normal lysosomal function by increasing the intralysosomal pH (38), completely prevented this degradation, whereas chloroquine alone did not affect OATP2B1 protein content (Fig. 5*D*).

Mechanism of OATP2B1 Internalization—Several pathways have been implicated in internalization of plasma membrane proteins. The main and thus most extensively studied endocytotic routes are caveolin/lipid raft and clathrin-mediated pathways. To investigate the involvement of these processes in PMA-induced OATP2B1 internalization a siRNA-based knock-down of the main contributors of these processes, caveolin-1 (Cav1) and CHC, was performed. Western blot analyses confirmed the knock-down (Cav1, 20 ± 9% of control after 48 h; CHC, 26 ± 9% of control after 72 h) (Fig. 6*A*). Confocal microscopy analyses demonstrated that depletion of

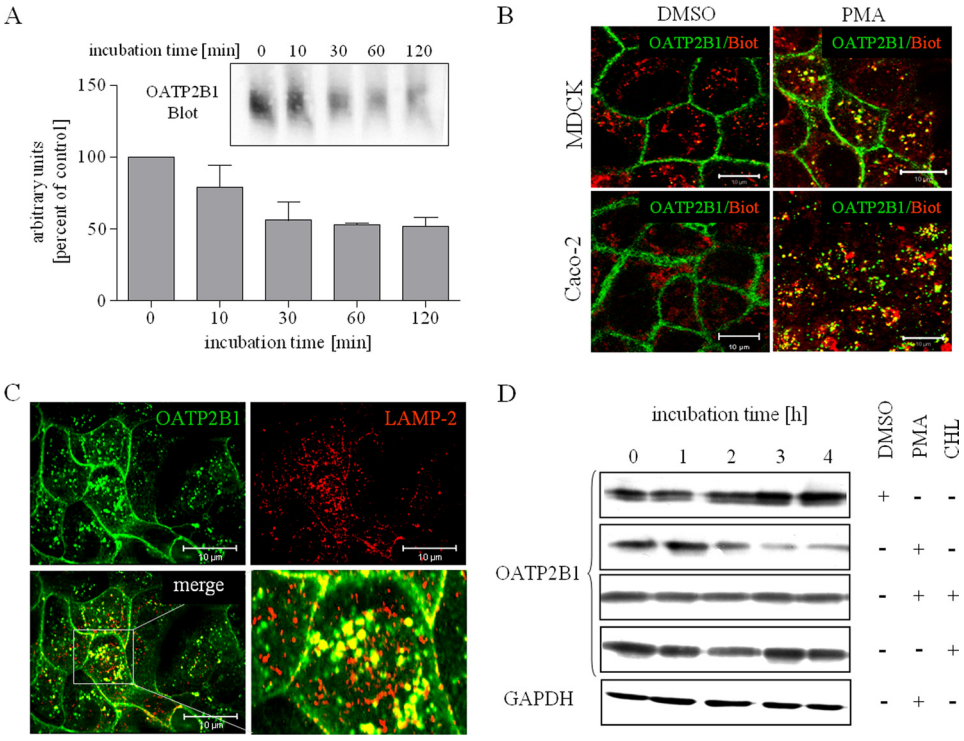

FIGURE 5. **Fate of OATP2B1.** *A*, for cell surface biotinylation, MDCKII-OATP2B1 cells were treated with PMA (100 nM) at 37 °C for the indicated times and biotinylated for 1 h at 4 °C. After cell lysis biotinylated proteins were pulled down by Neutravidin-agarose and analyzed for OATP2B1 expression by Western blot (*inset*). Arbitrary units were calculated from two independent experiments. Data represent mean + S.D. *B*, fluorescence-based internalization assay: MDCKII-OATP2B1 cells as well as Caco-2 cells were reversibly biotinylated. Following treatment with solvent or PMA (100 nM, 1 h) cell surface biotin was cleaved off using glutathione. After fixation cells were probed with the OATP2B1/r antibody (*green*) and intracellular biotin was stained with fluorescein isothiocyanate-labeled streptavidin (*red*) as described under "Experimental Procedures." *C*, colocalization with LAMP-2. Immunofluorescence staining of OATP2B1 and LAMP-2 performed in MDCKII-OATP2B1 cells after a 2-h treatment with 100 nM PMA showed partial colocalization of OATP2B1 and LAMP-2 (yellow fluorescence). *D*, lysosomal degradation of OATP2B1 following PMA treatment. MDCKII-OATP2B1 cells were preincubated with 100 μM chloroquine (*CHL*), which inhibits lysosomal degradation by increasing the intralysosomal pH, or DMSO for 30 min, before cells were treated with 100 nM PMA or vehicle in the continuous presence of preincubation agent for the time intervals indicated. Afterward, cells were lysed and 50 μg of protein were loaded on a 7.5% SDS-PAGE gel. Representative immunoblots of OATP2B1 in total cell lysates are shown. Glyceraldehyde-3-phosphate dehydrogenase (*GAPDH*) staining is given for incubation with 100 nM PMA.

Cav-1 did not affect OATP2B1 localization as well as intracellular accumulation following PMA treatment. However, CHC knock-down dramatically impaired plasma membrane localization even in the absence of PMA, suggesting that CHC is involved in general trafficking processes of OATP2B1 (Fig. 6*B*). This general finding for CHC knock-down could be verified by Western blot analysis of the cell surface fraction as well as on a functional level (Fig. 6*C*). None of these treatments had an effect on E-cadherin, which was studied as a control plasma membrane protein (data not shown).

Although these findings indicated an involvement of CHC in trafficking of OATP2B1 they also demonstrated that the knock-down is not useful to study the involvement of CHC in PKC-mediated internalization of OATP2B1. Therefore, we used another approach to differentiate between caveolin/lipid raft-dependent and clathrin-mediated mechanisms based on their sensitivity to pharmacological inhibition. To disrupt caveolin-mediated endocytosis MDCKII-OATP2B1 cells were preincubated with the cholesterol-disrupting agents filipin and nystatin, which have previously been demonstrated to inhibit caveolin-

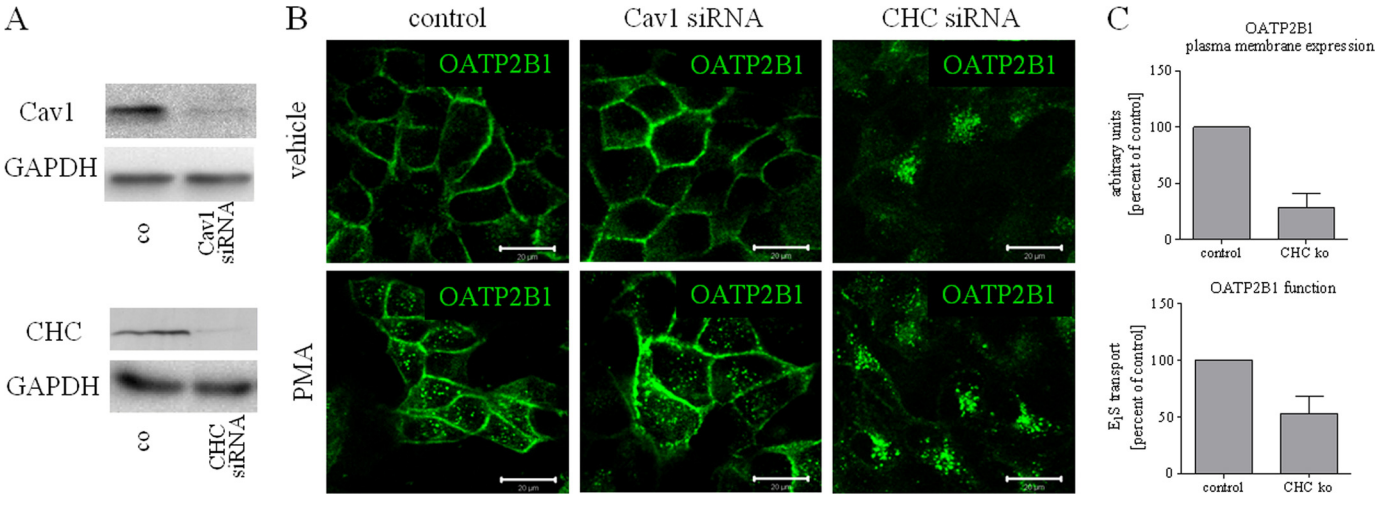

FIGURE 6. **Influence of caveolin and clathrin knock-down on OATP2B1 internalization.** *A*, knock-down of clathrin heavy chain and caveolin-1: MDCKII-OATP2B1 cells transfected with or without CHC and Cav1 siRNA for 72 or 48 h, respectively, were lysed and subjected to immunoblot assays. Detection of glyceraldehyde-3-phosphate dehydrogenase (*GAPDH*) was used as a control for protein loading. *B*, control as well as Cav1- and CHC-depleted MDCKII-OATP2B1 cells were incubated for 1 h at 37 °C in the presence or absence of PMA (100 nM), fixed, and probed with the OATP2B1/r antibody. Data shown are representative for three independent experiments. The *bar* represents 20 μM. *C*, influence of CHC knock-down on function and localization of OATP2B1: MDCKII-OATP2B1 cells were transfected with CHC siRNA and cell surface biotinylation (*upper panel*) as well as analysis of E_1S uptake (*lower panel*) were performed as described in the legends to Figs. 1*A* and 4*A*. Data represent two independent experiments (mean + S.D.).

and lipid raft-dependent endocytosis in MDCKII cells (33). Inhibition of clathrin-mediated processes was achieved by acidification of the cytosol by acetic acid or incubation with hypertonic medium, which prevent proper formation or budding of the clathrin lattice at the plasma membrane (39). To demonstrate the effect of these internalization inhibitors on endocytosis we transiently transfected MDCKII-OATP2B1 cells with the hTfR, which is constitutively internalized via clathrin-dependent processes (40). As expected, calculation of the ratio between expression in the plasma membrane and the cytoplasmatic compartment revealed that only sucrose and acetic acid treatment were able to prevent internalization of the hTfR. While in control, nystatin-, and filipin-treated cells about 60% of the hTfR was localized intracellularly, inhibition of clathrin-mediated endocytosis decreased the intracellular accumulation to 20% (Fig. 7, *A* and *B*). Furthermore, following PMA stimulation we observed a colocalization of hTfR and OATP2B1 in the intracellular compartments, suggesting that the transport protein is internalized via clathrin-coated pits. (Fig. 7*C*).

As expected from caveolin knock-down experiments neither filipin nor nystatin affected endocytosis of OATP2B1 after PMA stimulus, whereas inhibition of clathrin-dependent endocytosis prevented the PMA-mediated retrieval of OATP2B1 from the plasma membrane but not of E-cadherin. None of the substances itself altered plasma membrane localization of the transporter (Fig. 8*A*). Quantitation of these immunofluorescence

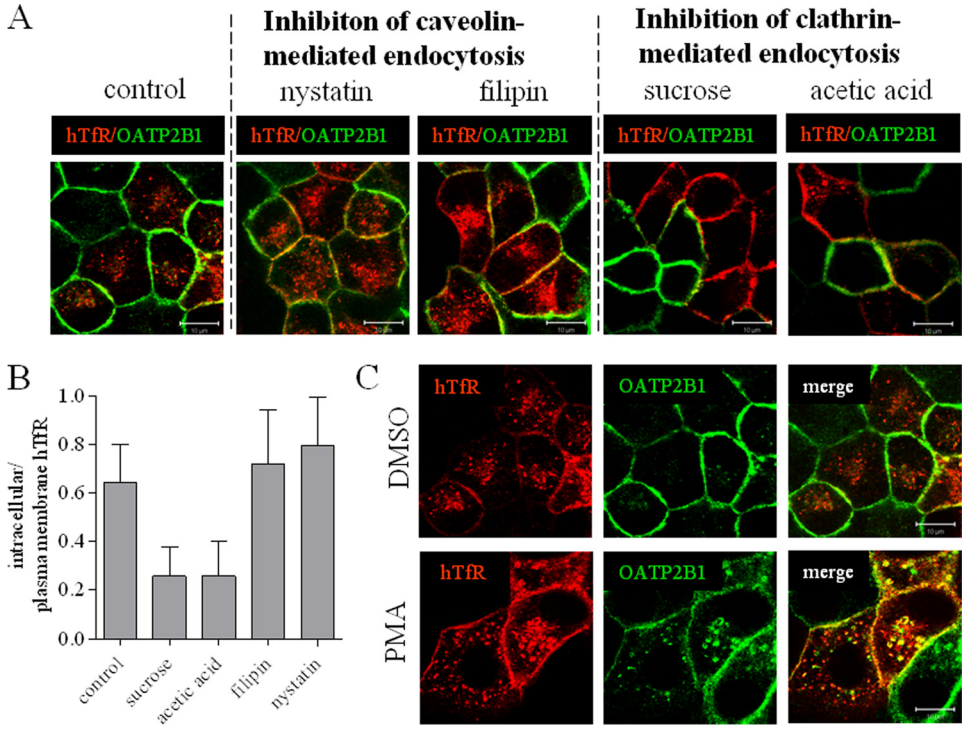

FIGURE 7. **Inhibition of caveolin- or clathrin-mediated endocytosis on hTfR expression.** *A*, to demonstrate an effect of internalization inhibitors, MDCKII-OATP2B1 cells cotransfected with YFP-tagged transferrin receptor (*hTfR*) were subjected to chemical or pharmacological treatment influencing endocytotic processes. To inhibit caveolin-mediated endocytosis MDCKII-OATP2B1 cells were incubated with 5 μg/ml of filipin or 25 μM nystatin for 30 min in growth medium; to inhibit clathrin-mediated endocytosis cells were treated with 0.45 M sucrose for 30 min or with 10 mM acetic acid in growth medium for 10 min prior to treatment with PMA (100 nM) or vehicle in the continuous presence of the inhibitors for 1 h. Afterward, cells were fixed and stained with the OATP2B1/r antibody. *B*, hTfR receptor expression in the plasma membrane and cytosol after treatment with inhibitors of clathrin- and caveolin-mediated endocytosis was quantitated using the LSM510 image browser (mean ± S.D., $n = 18$ cells). *C*, colocalization of hTfR and OATP2B1: hTfR-transfected MDCKII-OATP2B1 cells were treated with PMA (100 nM) or DMSO for 1 h and probed with the OATP2B1/r antibody. hTfR is given in *red*, OATP2B1 in *green*. Colocalization of both proteins is highlighted in *yellow*.

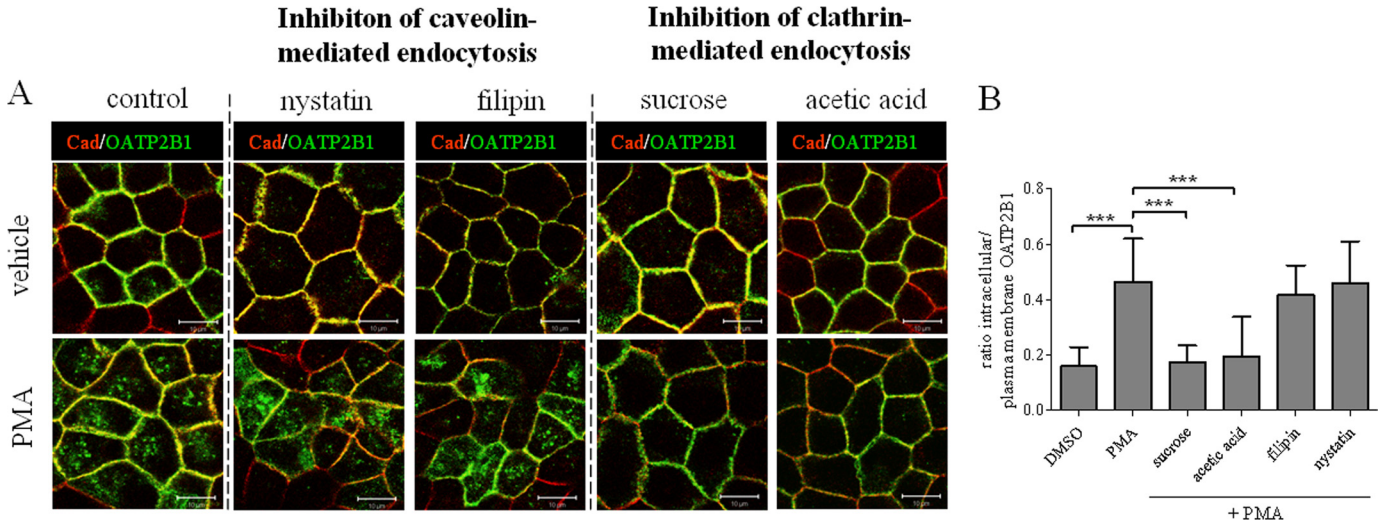

FIGURE 8. **Effect of internalization inhibitors on OATP2B1 localization.** *A*, MDCKII-OATP2B1 cells were incubated with 100 nM PMA or DMSO in the presence of internalization inhibitors for 1 h as described in the legend to Fig. 7*A*. Afterward, cells were fixed and stained with the OATP2B1/r and E-cadherin antibody. E-cadherin is given in *red*, OATP2B1 in *green*. The *bar* represents 10 μM. *B*, OATP2B1 expression in PMA or control-treated cells was quantified for intracellular accumulation. Values of are given as the ratio between intracellular and plasma membrane expression (mean ± S.D., $n = 18$ cells). ***, $p < 0.001$.

data demonstrated that sucrose and acetic acid treatment, but not inhibition of caveolin-dependent processes, were able to reduce intracellular accumulation of OATP2B1 to control levels following PKC activation (Fig. 8*B*).

DISCUSSION

The function of drug transporters of the ABC or SLC superfamily is mainly determined by the amount of carrier protein expressed at the plasma membrane. Aside from well characterized transcriptional modifications, transport activity can be influenced by post-translational modifications resulting in altered localization and/or activity of the carrier protein. In the present study, we describe a rapid regulation of the organic anion transporting polypeptide 2B1 (OATP2B1) by internalization following PKC activation.

OATP2B1 is a cellular uptake carrier for a growing number of drugs including statins or the oral antidiabetic glibenclamide, but it is also involved in the transport of endogenous compounds like sulfated steroid conjugates (12–14, 18–20). Its ubiquitous expression in association with a wide spectrum of substrates implicates physiological, as well as pharmacological relevance for distribution of both drugs and endogenous compounds.

While neither direct nor indirect activation of PKA affected transport activity, treatment with the PKC activator PMA resulted in decreased OATP2B1-mediated transport. This effect was time-dependent with a rapid onset (significant effects after 20 min) and a maximum after 2 h. Interestingly, prolonged incubation resulted in a lower inhibition. Similar recovery phenomena after long-term treatment with phorbol esters have been described for the activity of the human cation transporter hCAT1, as well as PMA-mediated multidrug resistance related protein 2 retrieval from the apical membrane of HepG2 cells (41). Several mechanisms have been proposed to explain those time profiles including transcriptional down-regulation, degradation, as well as altered distribution and hence activity of PKC (42–44). This involvement of PKC in regulation of transport proteins is consistent with our finding that PKC is involved in decreased OATP2B1-mediated transport as demonstrated by a partial reversal of the PMA-mediated inhibition by pretreatment with the PKC inhibitor BIM-I (45).

In the present study we show that inhibition of OATP2B1-mediated E_1S transport by PMA is kinetically revealed as a change in V_{max}. Because substrate affinity remained statistically unchanged, this suggests either attenuated plasma membrane expression by changes of localization and/or protein synthesis or even a direct effect on the transporters mode of action. For a number of biologically important proteins including the epidermal growth factor receptor (46) or chemokine receptors (46), as well as many neurotransmitter transporters (reviewed in Ref. 47), inhibition of transport function was associated with a significant loss of cell surface expression. Indeed, we observed a decreased plasma membrane and enhanced intracellular localization of OATP2B1. Interestingly, prolonged incubation with PMA resulted in a recovery of plasma membrane OATP2B1 supporting the notion of a desensitization against PKC stimulation and recovery of function.

Because even a 20-min exposure to PMA resulted in a significant inhibition of OATP2B1 transport activity we assumed that internalization rather than inhibition of protein synthesis is the underlying mechanism. This is supported by immunofluorescence stainings, biotinylation experiments, and live-cell image analysis, which correlated with the observed decrease of OATP2B1 transport activity following PKC activation. Taken together, these approaches reveal that stimulation by PMA results in sequestration of the protein from the plasma membrane into intracellular compartments. Colocalization studies with internalized biotin-labeled plasma membrane proteins indicate that OATP2B1 is internalized from the plasma membrane rather than accumulated by decreased trafficking to the plasma membrane.

Similar internalization effects were obtained for Caco-2 cells, which have previously been shown to endogenously express OATP2B1 (48, 49), as well as human placenta employing an *ex vivo* perfusion study. Therefore, the internalization was not cell type-specific or due to protein overexpression.

Because several studies indicate that the internalization of proteins following PKC activation is associated with phosphorylation, we tested whether OATP2B1 is phosphorylated in response to PMA treatment. Our data demonstrate that OATP2B1 in MDCKII cells is already phosphorylated under basal conditions. Although internalization of OATP2B1 in response to PKC activation was accompanied by a 2-fold increase in phosphorylation, mutation of 17 putative phosphorylation sites did not inhibit PMA-mediated internalization, suggesting that phosphorylation of these amino acids is not the underlying reason for PKC-mediated internalization. Therefore, other mechanism like dileucine- or tyrosine-based trafficking motifs as well as adaptor proteins or atypical phosphorylation sites might be involved in this process. Although it is a prevailing assumption that phosphorylation is required for PMA-induced internalization, several studies also demonstrate PMA-activated PKC-mediated internalization of plasma membrane proteins independent of putative phosphorylation sites (25, 50).

Following internalization, OATP2B1 can either recycle back to the plasma membrane or undergo proteosomal or lysosomal degradation. The observation that OATP2B1 colocalizes with LAMP-2 and the total transporter expression decreases time dependently suggests the latter pathway. This assumption could be verified by Western blot analysis employing chloroquine, which inhibits lysosomal degradation by elevating intralysosomal pH (38) and was able to prevent degradation of OATP2B1. Degradation processes also explain that recovery of OATP2B1-mediated transport inhibition by PKC modulation required more than 10 h in washout experiments.

We further addressed the question, whether the internalization of OATP2B1 is mediated by clathrin- or caveolae/lipid raft-mediated processes, which both have been described in intracellular retrieval of transport proteins like the dopamine transporter DAT (51) or the norepinephrine transporter hNET (52), respectively.

In our study, neither Cav1 knock-down nor inhibition of caveolae/lipid raft-mediated endocytosis by filipin or nystatin blocked the PMA-mediated alteration of OATP2B1

localization. Interestingly, knock-down of CHC resulted in an intracellular OATP2B1 accumulation independent from PMA treatment, whereas the control plasma membrane protein E-cadherin was not affected. As expected, the disturbed plasma membrane expression of OATP2B1 resulted in decreased transport function of the protein.

To circumvent the effects of the CHC knock-down on OATP2B1 trafficking and sorting, we used a second approach to inhibit clathrin-dependent endocytosis. Acidification of the cytosol with acetic acid or incubation with hypertonic medium, which prevent formation of the clathrin lattice at the plasma membrane and inhibit internalization of a number of membrane proteins (32, 39, 53, 54) almost completely abolished the PMA-mediated retrieval of OATP2B1 from the plasma membrane. Endocytosis of the transferrin receptor, which is a marker for clathrin-mediated endocytosis, was also inhibited under these conditions, but not by inhibitors of caveolin-mediated processes as mentioned before.

The divergent results of CHC knock-down and chemical interference are contradictory at first sight; however, clathrin-coated vesicles are not only major carriers from the plasma membrane but are also involved in trafficking of proteins from the trans-Golgi network to the plasma membrane. A recent study by Deborde *et al.* (55) highlighted the role of clathrin in trafficking of basolateral proteins demonstrating that clathrin heavy chain depletion in MDCK cells slows the exit of basolateral proteins from the Golgi and leads to a missorting into apical vesicles. Taken together, our data indicate that CHC is not only involved in PKC-mediated internalization but also in general trafficking of OATP2B1.

PKC activation has been described in response to various stimuli and under numerous pathophysiological conditions. For example, it has been shown that PKC isozymes are commonly dysregulated in prostate, breast, colon, pancreatic, liver, and kidney cancer (reviewed in Ref. 56). This expression also serves as a predictor of treatment outcome (57, 58). Taken into account that OATP expression has been demonstrated in cancer (7, 8, 10, 59) and several anti-cancer drugs like irinotecan, methotrexate, or paclitaxel are substrates of human OATPs (reviewed in Ref. 9), modulation of transport activity by PKC may affect the intracellular concentration of these substances and hence treatment outcome.

Regulation of protein function by post-translational modifications may also be of special importance in platelets, because these anucleated cells only have limited means to regulate protein expression on a transcriptional level. Indeed, it has been shown that PKC is involved in key steps in platelet activation and aggregation. Only recently, we detected OATP2B1 in these structures and could demonstrate the uptake of the OATP2B1 substrate atorvastatin (11).

The idea that PKC activation influences transport processes is highlighted by a recent publication of Crocenzi *et al.* (60), which investigated the influence of protein kinase C isoforms on estradiol 17β-D-glucuronide (E_2G)-induced acute cholestasis. They demonstrated that E_2G activates PKCα in primary cultured rat hepatocytes and induces retrieval of Mrp2 and Bsep from the apical membrane, which normally provide the driving force for osmotic bile formation. E_2G-induced decrease in bile flow as well as altered localization of the transport proteins could be prevented by PKC inhibition.

Furthermore, it has been shown that besides E_2G, other steroid hormones like DHEA are also able to activate PKC (61). The sulfated metabolite of DHEA, DHEAS, serves as a major precursor molecule for the production of estrogens in the placenta. In contrast to the ovaries, which are able to generate estrogens by direct transformation of cholesterol, the placenta is highly dependent on uptake of precursor molecules from fetal or maternal circulation due to the lack of CYP17, which converts progesterone to DHEA (62). Recently, it has been shown that DHEAS is a substrate of OATP2B1, and it has been suggested by us and others that OATP2B1, which is expressed in the basolateral membrane of the placenta, is involved in uptake of this precursor molecule (29, 63). Down-regulation of OATP2B1 transport by PKC-mediated internalization as shown in the placenta employing an *ex vivo* perfusion model could therefore serve as a negative feedback mechanism limiting the uptake of precursors and hence the production of estrogens.

Taken together, the present study provides information on a new, rapid regulatory mechanism for human OATP-mediated transport processes, which can influence physiological as well as pharmacokinetic functions of this transport protein. *Ex vivo* perfusion of human placenta suggests that our *in vitro* findings also translate into biological systems.

Acknowledgments—We acknowledge the excellent technical assistance by Tina Sonnenberger, Bärbel Uecker, and Kerstin Böttcher (Department of Pharmacology, Ernst Moritz Arndt University, Greifswald, Germany).

REFERENCES

1. Iwai, M., Suzuki, H., Ieiri, I., Otsubo, K., and Sugiyama, Y. (2004) *Pharmacogenetics* **14,** 749–757
2. Tirona, R. G., Leake, B. F., Merino, G., and Kim, R. B. (2001) *J. Biol. Chem.* **276,** 35669–35675
3. Tachibana-Iimori, R., Tabara, Y., Kusuhara, H., Kohara, K., Kawamoto, R., Nakura, J., Tokunaga, K., Kondo, I., Sugiyama, Y., and Miki, T. (2004) *Drug Metab. Pharmacokinet.* **19,** 375–380
4. Deng, J. W., Song, I. S., Shin, H. J., Yeo, C. W., Cho, D. Y., Shon, J. H., and Shin, J. G. (2008) *Pharmacogenet. Genomics* **18,** 424–433
5. Link, E., Parish, S., Armitage, J., Bowman, L., Heath, S., Matsuda, F., Gut, I., Lathrop, M., and Collins, R. (2008) *N. Engl. J. Med.* **359,** 789–799
6. Niemi, M., Pasanen, M. K., and Neuvonen, P. J. (2006) *Clin. Pharmacol. Ther.* **80,** 356–366
7. Hamada, A., Sissung, T., Price, D. K., Danesi, R., Chau, C. H., Sharifi, N., Venzon, D., Maeda, K., Nagao, K., Sparreboom, A., Mitsuya, H., Dahut, W. L., and Figg, W. D. (2008) *Clin. Cancer Res.* **14,** 3312–3318
8. Lee, W., Belkhiri, A., Lockhart, A. C., Merchant, N., Glaeser, H., Harris, E. I., Washington, M. K., Brunt, E. M., Zaika, A., Kim, R. B., and El-Rifai, W. (2008) *Cancer Res.* **68,** 10315–10323
9. Hagenbuch, B., and Gui, C. (2008) *Xenobiotica* **38,** 778–801
10. Al Sarakbi, W., Mokbel, R., Salhab, M., Jiang, W. G., Reed, M. J., and Mokbel, K. (2006) *Anticancer Res.* **26,** 4985–4990
11. Niessen, J., Jedlitschky, G., Grube, M., Bien, S., Schwertz, H., Ohtsuki, S., Kawakami, H., Kamiie, J., Oswald, S., Starke, K., Strobel, U., Siegmund, W., Rosskopf, D., Greinacher, A., Terasaki, T., and Kroemer, H. K. (2009) *Drug Metab. Dispos.* **37,** 1129–1137
12. Grube, M., Köck, K., Oswald, S., Draber, K., Meissner, K., Eckel, L., Böhm, M., Felix, S. B., Vogelgesang, S., Jedlitschky, G., Siegmund, W., Warzok, R., and Kroemer, H. K. (2006) *Clin. Pharmacol. Ther.* **80,** 607–620

13. Kobayashi, D., Nozawa, T., Imai, K., Nezu, J., Tsuji, A., and Tamai, I. (2003) *J. Pharmacol. Exp. Ther.* **306,** 703–708
14. Kullak-Ublick, G. A., Ismair, M. G., Stieger, B., Landmann, L., Huber, R., Pizzagalli, F., Fattinger, K., Meier, P. J., and Hagenbuch, B. (2001) *Gastroenterology* **120,** 525–533
15. St-Pierre, M. V., Hagenbuch, B., Ugele, B., Meier, P. J., and Stallmach, T. (2002) *J. Clin. Endocrinol. Metab.* **87,** 1856–1863
16. Vaidyanathan, S., Camenisch, G., Schuetz, H., Reynolds, C., Yeh, C. M., Bizot, M. N., Dieterich, H. A., Howard, D., and Dole, W. P. (2008) *J. Clin. Pharmacol.* **48,** 1323–1338
17. Grube, M., Köck, K., Karner, S., Reuther, S., Ritter, C. A., Jedlitschky, G., and Kroemer, H. K. (2006) *Mol. Pharmacol.* **70,** 1735–1741
18. Nozawa, T., Imai, K., Nezu, J., Tsuji, A., and Tamai, I. (2004) *J. Pharmacol. Exp. Ther.* **308,** 438–445
19. Satoh, H., Yamashita, F., Tsujimoto, M., Murakami, H., Koyabu, N., Ohtani, H., and Sawada, Y. (2005) *Drug Metab. Dispos.* **33,** 518–523
20. Tamai, I., Nozawa, T., Koshida, M., Nezu, J., Sai, Y., and Tsuji, A. (2001) *Pharm. Res.* **18,** 1262–1269
21. Cheng, X., Maher, J., Dieter, M. Z., and Klaassen, C. D. (2005) *Drug Metab. Dispos.* **33,** 1276–1282
22. Rost, D., Kopplow, K., Gehrke, S., Mueller, S., Friess, H., Ittrich, C., Mayer, D., and Stiehl, A. (2005) *Eur. J. Clin. Invest.* **35,** 635–643
23. Jigorel, E., Le Vee, M., Boursier-Neyret, C., Parmentier, Y., and Fardel, O. (2006) *Drug Metab. Dispos.* **34,** 1756–1763
24. Stedman, C. A., Liddle, C., Coulter, S. A., Sonoda, J., Alvarez, J. G., Moore, D. D., Evans, R. M., and Downes, M. (2005) *Proc. Natl. Acad. Sci. U.S.A.* **102,** 2063–2068
25. Wolff, N. A., Thies, K., Kuhnke, N., Reid, G., Friedrich, B., Lang, F., and Burckhardt, G. (2003) *J. Am. Soc. Nephrol.* **14,** 1959–1968
26. Zhang, Q., Hong, M., Duan, P., Pan, Z., Ma, J., and You, G. (2008) *J. Biol. Chem.* **283,** 32570–32579
27. Guo, G. L., and Klaassen, C. D. (2001) *J. Pharmacol. Exp. Ther.* **299,** 551–557
28. Sun, A. Q., Ponamgi, V. M., Boyer, J. L., and Suchy, F. J. (2008) *Pharm. Res.* **25,** 463–474
29. Grube, M., Reuther, S., Meyer zu Schwabedissen, H., Köck, K., Draber, K., Ritter, C. A., Fusch, C., Jedlitschky, G., and Kroemer, H. K. (2007) *Drug Metab. Dispos.* **35,** 30–35
30. May, K., Minarikova, V., Linnemann, K., Zygmunt, M., Kroemer, H. K., Fusch, C., and Siegmund, W. (2008) *Drug Metab. Dispos.* **36,** 740–744
31. Grube, M., Meyer zu Schwabedissen, H. E., Präger, D., Haney, J., Möritz, K. U., Meissner, K., Rosskopf, D., Eckel, L., Böhm, M., Jedlitschky, G., and Kroemer, H. K. (2006) *Circulation* **113,** 1114–1122
32. Hansen, S. H., Sandvig, K., and van Deurs, B. (1993) *J. Cell Biol.* **121,** 61–72
33. Rothberg, K. G., Heuser, J. E., Donzell, W. C., Ying, Y. S., Glenney, J. R., and Anderson, R. G. (1992) *Cell* **68,** 673–682
34. Blom, N., Gammeltoft, S., and Brunak, S. (1999) *J. Mol. Biol.* **294,** 1351–1362
35. Iakoucheva, L. M., Radivojac, P., Brown, C. J., O'Connor, T. R., Sikes, J. G., Obradovic, Z., and Dunker, A. K. (2004) *Nucleic Acids Res.* **32,** 1037–1049
36. Xue, Y., Ren, J., Gao, X., Jin, C., Wen, L., and Yao, X. (2008) *Mol. Cell. Proteomics* **7,** 1598–1608
37. Maxfield, F. R., and McGraw, T. E. (2004) *Nat. Rev. Mol. Cell. Biol.* **5,** 121–132
38. Lie, S. O., and Schofield, B. (1973) *Biochem. Pharmacol.* **22,** 3109–3114
39. Heuser, J. E., and Anderson, R. G. (1989) *J. Cell Biol.* **108,** 389–400
40. Sandvig, K., Olsnes, S., Petersen, O. W., and van Deurs, B. (1987) *J. Cell Biol.* **105,** 679–689
41. Gräf, P., Förstermann, U., and Closs, E. I. (2001) *Br. J. Pharmacol.* **132,** 1193–1200
42. Goode, N. T., Hajibagheri, M. A., and Parker, P. J. (1995) *J. Biol. Chem.* **270,** 2669–2673
43. Hepler, J. R., Earp, H. S., and Harden, T. K. (1988) *J. Biol. Chem.* **263,** 7610–7619
44. Leontieva, O. V., and Black, J. D. (2004) *J. Biol. Chem.* **279,** 5788–5801
45. Toullec, D., Pianetti, P., Coste, H., Bellevergue, P., Grand-Perret, T., Ajakane, M., Baudet, V., Boissin, P., Boursier, E., and Loriolle, F. (1991) *J. Biol. Chem.* **266,** 15771–15781
46. Rothman, J. E., and Fine, R. E. (1980) *Proc. Natl. Acad. Sci. U.S.A.* **77,** 780–784
47. Melikian, H. E. (2004) *Pharmacol. Ther.* **104,** 17–27
48. Sai, Y., Kaneko, Y., Ito, S., Mitsuoka, K., Kato, Y., Tamai, I., Artursson, P., and Tsuji, A. (2006) *Drug Metab. Dispos.* **34,** 1423–1431
49. Seithel, A., Karlsson, J., Hilgendorf, C., Björquist, A., and Ungell, A. L. (2006) *Eur. J. Pharm. Sci.* **28,** 291–299
50. Granas, C., Ferrer, J., Loland, C. J., Javitch, J. A., and Gether, U. (2003) *J. Biol. Chem.* **278,** 4990–5000
51. Sorkina, T., Hoover, B. R., Zahniser, N. R., and Sorkin, A. (2005) *Traffic* **6,** 157–170
52. Jayanthi, L. D., Annamalai, B., Samuvel, D. J., Gether, U., and Ramamoorthy, S. (2006) *J. Biol. Chem.* **281,** 23326–23340
53. Chow, C. W., Khurana, S., Woodside, M., Grinstein, S., and Orlowski, J. (1999) *J. Biol. Chem.* **274,** 37551–37558
54. Antonescu, C. N., Díaz, M., Femia, G., Planas, J. V., and Klip, A. (2008) *Traffic* **9,** 1173–1190
55. Deborde, S., Perret, E., Gravotta, D., Deora, A., Salvarezza, S., Schreiner, R., and Rodriguez-Boulan, E. (2008) *Nature* **452,** 719–723
56. Ali, A. S., Ali, S., El-Rayes, B. F., Philip, P. A., and Sarkar, F. H. (2009) *Cancer Treat. Rev.* **35,** 1–8
57. Assender, J. W., Gee, J. M., Lewis, I., Ellis, I. O., Robertson, J. F., and Nicholson, R. I. (2007) *J. Clin. Pathol.* **60,** 1216–1221
58. Pan, Q., Bao, L. W., Kleer, C. G., Sabel, M. S., Griffith, K. A., Teknos, T. N., and Merajver, S. D. (2005) *Cancer Res.* **65,** 8366–8371
59. Wlcek, K., Svoboda, M., Thalhammer, T., Sellner, F., Krupitza, G., and Jaeger, W. (2008) *Cancer Biol. Ther.* **7,** 1450–1455
60. Crocenzi, F. A., Sánchez Pozzi, E. J., Ruiz, M. L., Zucchetti, A. E., Roma, M. G., Mottino, A. D., and Vore, M. (2008) *Hepatology* **48,** 1885–1895
61. Alzamora, R., and Harvey, B. J. (2008) *Steroids* **73,** 885–888
62. Voutilainen, R., and Miller, W. L. (1986) *J. Clin. Endocrinol. Metab.* **63,** 1145–1150
63. Pizzagalli, F., Varga, Z., Huber, R. D., Folkers, G., Meier, P. J., and St-Pierre, M. V. (2003) *J. Clin. Endocrinol. Metab.* **88,** 3902–3912